Journal of Computational Applied Mechanics 2025, 56(4): 776-790

DOI: 10.22059/jcamech.2025.398637.1551

RESEARCH PAPER

Effect of Varying Thermal Conductivity on MHD Micropolar Fluid Flow Based on Cattaneo-Christov Heat Flux Model over an Exponentially Extended Stretching Curved Surface

Sultan Z Alamri [a], Ambreen A. Khan [b], Iqra Nasreen [b], Rahmat Ellahi [b, c, *]

[a] *Faculty of Science, Taibah University, Madinah Al Munawwarha Saudi Arabia*
[b] *Department of Mathematics & Statistics, International Islamic University, Islamabad Pakistan*
[c] *Center for Modeling & Computer Simulation, Research Institute, King Fahd University of Petroleum & Minerals, Dhahran-31261, Saudi Arabia*

Abstract

This study investigates the magnetohydrodynamic (MHD) flow of a micropolar fluid over an exponentially extended stretching curved surface. The boundary layer flow along with temperature-dependent thermal conductivity is also taken into account. The Cattaneo-Christov heat flux model is used for energy equation. The curvilinear coordinates are used in the formation of flow equations. The governing non-linear partial differential equations (PDEs) are transformed into coupled non-linear ordinary different equations (ODEs) by appropriate transformations. The resulting ODEs are solved numerically using the ND-solve method in Mathematica. Graphs are plotted to explore the impacts of key parameters on microrotation, temperature, and velocity. Results show that increasing curvature leads to higher velocity and lower temperature, with potential applications in polymer processing and waste treatment. A comparison has been made with the existing literature as a limited case of present study to validate the results.

Keywords: Cattaneo-Christov Heat Transfer; Variable Thermal Conductivity; Curved Stretching Surface; Micropolar MHD flow; Non-Fourier Energy Equation; exponentially stretching sheet.

1. Introduction

Non-Newtonian fluids have a vast number of applications in engineering and industrial purposes because of their complex and nonlinear equations [1-8]. These fluids will not be described by a single relation. Eringen proposed the theory of non-Newtonian fluid known as micropolar fluid [9-11]. The behavior of this fluid is completely dissimilar from other non-Newtonian fluids because it shows microscopic properties [12]. The micropolar fluid considered the rotation of the fluid, which is represented by microrotation property. It has a wide variety of applications in blood flow, liquid composite modeling, polymer melts, liquid crystals, and suspensions. A lot of researchers have worked on solving these

* Corresponding author. (R. Ellahi): *E-mail address:* rahmatellahi@yahoo.com

governing equations of micropolar fluid in different coordinates. Turkyilmazoglu [13] has examined the micropolar fluid on an extended sheet. Zadeh et al. [14] has described numerically the movement of nanofluid and heat transfer over the stretching sheet, which is influenced by microorganisms. Ahmed et al. [15] has studied micropolar fluid flowing through a hollow cylinder with mixed convection. Elgazery and Nasser [16] have examined the micropolar nanofluid flow through a cylinder which is placed horizontally.

The flow of liquid over a curved sheet has fascinated many researchers due to its wide range of applications in designs of aerofoils to reduce the drag force in vehicles, in the construction of dams, bridges, and pipelines, and also in biomedical and chemical engineering. Ghobadi and Muzychka [17] have extended the work on motion of Newtonian liquid in coiled, circular curved tubes under the impact of pressure drop relations. Khan et al. [18] have inspected the transformed equations of micropolar fluid with modified Fourier law flowing in curved channel. Muhammad et al. [19] investigated the flow of Darcy–Forchheimer Newtonian liquid in an exponentially extended curved surface. Kempannagari et al. [20] examined the stagnation point motion of non-Newtonian liquid over a curved surface, which is also extended exponentially. Shi et al. [21] numerically described the micropolar fluid moving in an exponentially extended curved surface using the Keller box method. Kumar et al. [22] investigated the free convective stagnation motion of non-Newtonian fluid in a curved surface that is extended exponentially.

The thermal conductivity of various fluids is assumed to be constant. However, this assumption fails to give a realistic understanding of when internal resistance generates heat in many industrial operations. In these industrial processes, physical phenomena like thermal conductivity, which are primarily exploited in the lubrication theory used in fluid bearing design, significantly alter the temperature difference [23-26]. The temperature-dependent conductivity connection was used by several scientists for product refinement, including in viscometer and wear, for instance, Megahed et al. [27] deliberated the flow of an unsteady viscous fluid with thermal and variable fluid properties. Khan et al. [28] discussed the effect of an induced magnetic field on second grade fluid under the impact of variable thermal conductivity. Moreover, the Cattaneo-Christov heat flux model is particularly relevant when considering situations where heat transfer is rapid or the material has a significant thermal relaxation time [29, 30]. Furthermore, the effects of MHD on micropolar fluids significantly influence flow characteristics, heat transfer, and related phenomena. MHD introduces a Lorentz force, which can either enhance or oppose the fluid motion depending on the magnetic field strength and orientation. In micropolar fluids, the presence of micro-rotation adds another layer of complexity, affecting the overall behavior under MHD influence. In addition, MHD with thermal conductivity interact to influence fluid flow and heat transfer in various applications [31-33]. The interplay of these factors is crucial in areas like heat exchangers, nuclear reactors, and even space physics.

Based on the literature reviewed, no existing literature discussed the micropolar MHD fluid over an exponentially extended curved surface with viscous dissipation and variable thermal conductivity with Cattaneo-Christov heat flux model. The curvilinear coordinates are used in mathematical equations and the formation of flow equations. An appropriate transformation is first used to convert the nonlinear governing partial differential equations into non-linear ordinary differential equations and are then solved by the ND-solver command to get their solutions. Graphical illustration is presented to examine the role of significant parameters. A comparison has been made with the existing literature as a limited case of present study to validate the results and found in good agreement.

2. Mathematical Formulation

Consider the steady and incompressible micropolar fluid flow over a curved sheet which is an exponentially stretching. The sheet is stretching with velocity $u_w(s) = \alpha e^{\frac{s}{d}}$ along the s-direction, $(\alpha, d > 0)$ where reference length is represented by d and α is the initial stretching rate. Consider the curvilinear coordinate system (r, s), with r-axis perpendicular and s-axis in the direction of flow. Let R° represent the radius of a circle. Consider the constant magnetic field $\widetilde{B}_0$, which is applied in r direction. Let us assume the temperature distribution $T = T(r,s)$ and velocity distribution $\boldsymbol{V} = [v(r,s), u(r,s)]$. The temperature of the surface is T_w, where $T_w > T_\infty$ the ambient temperature of the fluid.

The governing equations of the fluid and energy, based on boundary layer approximations are as given below:

$$\frac{\partial}{\partial r}\left((\mathrm{r} + \mathrm{R}^\circ)\mathrm{v}\right) + \frac{\partial u}{\partial s}\mathrm{R}^\circ = 0, \tag{1}$$

$$\frac{\partial p}{\partial r} = \frac{\rho}{r+\mathrm{R}^\circ}u^2, \tag{2}$$

$$\left(v\frac{\partial u}{\partial r} + \frac{\mathrm{R}^\circ \mathrm{u}}{r+\mathrm{R}^\circ}\frac{\partial u}{\partial s} + \frac{\mathrm{uv}}{r+\mathrm{R}^\circ}\right)\rho = -\sigma\widetilde{B}_0^2 u - \frac{\mathrm{R}^\circ}{r+\mathrm{R}^\circ}\frac{\partial p}{\partial s} - \breve{k}\frac{\partial N}{\partial r}$$

$$+(\mu+\check{k})\left[\frac{\partial^2 u}{\partial r^2}+\frac{1}{r+\mathrm{R}^\circ}\frac{\partial u}{\partial r}-\frac{u}{(r+\mathrm{R}^\circ)^2}\right], \tag{3}$$

$$\rho j\left(v\frac{\partial N}{\partial r}+\frac{\mathrm{R}^\circ u}{r+\mathrm{R}^\circ}\frac{\partial N}{\partial s}\right)=\xi\left(\frac{\partial^2 N}{\partial r^2}+\frac{1}{r+\mathrm{R}^\circ}\frac{\partial N}{\partial r}\right)-\check{k}\left(2N+\frac{\partial u}{\partial r}+\frac{u}{r+\mathrm{R}^\circ}\right), \tag{4}$$

$$\left(v\frac{\partial T}{\partial r}+\frac{\mathrm{R}^\circ u}{r+\mathrm{R}^\circ}\frac{\partial T}{\partial s}\right)=\frac{\frac{\partial}{\partial r}\left(K(T)\frac{\partial T}{\partial r}\right)+\frac{\partial}{\partial s}\left(\frac{\mathrm{R}^{\circ 2}K(T)}{(r+\mathrm{R}^\circ)^2}\frac{\partial T}{\partial s}\right)-\frac{K(T}{r+\mathrm{R}^\circ)}\frac{\partial T}{\partial r}}{\rho c_p}+q^*$$

$$-\lambda\left(\begin{array}{c}v^2\frac{\partial^2 T}{\partial r^2}+\frac{\mathrm{R}^\circ u}{r+\mathrm{R}^\circ}\frac{\partial T}{\partial s}\frac{\partial u}{\partial r}+\frac{(\mathrm{R}^\circ u)^2}{(r+\mathrm{R}^\circ)^2}\frac{\partial^2 T}{\partial s^2}+\frac{\mathrm{R}^\circ u}{r+\mathrm{R}^\circ}\frac{\partial T}{\partial r}\frac{\partial v}{\partial s}\\ -v\frac{\partial T}{\partial r}\frac{\partial v}{\partial r}-\frac{\mathrm{R}^\circ uv}{r+\mathrm{R}^\circ}\frac{\partial T}{\partial r}+\frac{2\mathrm{R}^\circ uv}{r+\mathrm{R}^\circ}\frac{\partial^2 T}{\partial r\,\partial s}\end{array}\right). \tag{5}$$

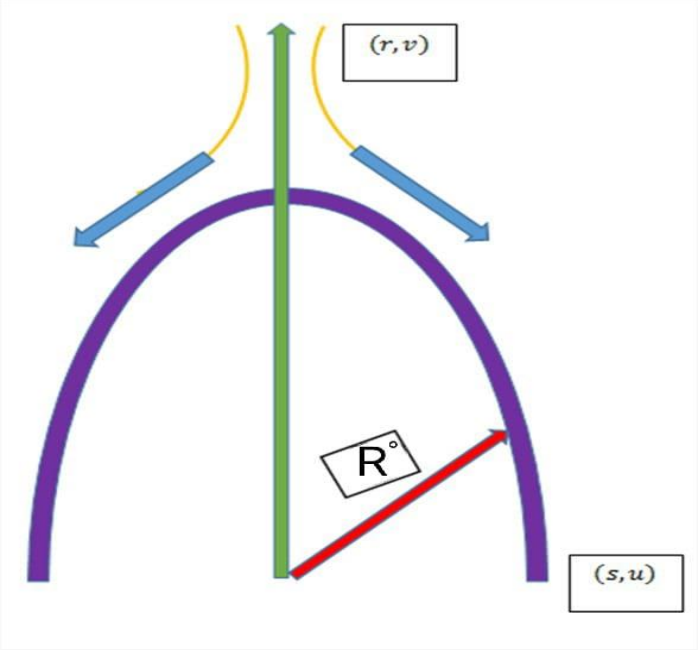

Fig. 1: The geometry of the problem.

The components of corresponding velocities is represented as (u, v) in direction (s, r) respectively. Likewise pressure is represented by p, ρ represents density, electrical conductivity is represented by σ, μ shows viscosity, N is microrotation parameter, c_p is heat capacitance, μ′ is kinematic viscosity, j is micro-inertia , $\check{k}$ is vortex viscosity, $\xi=\left(\mu+\frac{\check{k}}{2}\right)=\mu j\left(1+\frac{\beta}{2}\right)$ is spin gradient viscosity where $j=\frac{2dv}{\alpha e\frac{s}{d}}$, thermal relaxation time is denoted by λ.

The variable thermal conductivity is defined as below:

$$K(T)=k_\infty[1+c(T-T_\infty)]. \tag{6}$$

In which c is constant that varies according to nature of fluid, k_∞ the ambient thermal conductivity and β the material parameter. The term q^* represents a heat sink/source which as non-uniform is explained in the following equation:

$$q^*=K(T)u_w\frac{1}{2dv}\left(\hat{A}(T_w-T_\infty)f'+\hat{B}(T-T_\infty)\right). \tag{7}$$

If the variables $\hat{A}, \hat{B} > 0$ shows that heat is rising and $\hat{A}, \hat{B} < 0$ shows that heat is reducing.

The boundary conditions are given as

$$T = T_w, \qquad u = u_w(s) = \alpha e^{\frac{s}{d}} \ , N = -M_r \frac{\partial u}{\partial r}, v = 0, \qquad at \quad r = 0,$$

$$u \to 0, \frac{\partial u}{\partial r} \to 0, N \to 0, T \to T_\infty \quad as \quad r \to \infty, \tag{8}$$

where $M_r, 0 \le M_r \le 1$ shows the microrotation parameter. As microelements of the fluid cannot spin near the wall because the concentration of fluid is very high so $M_r = 0$.

3. Solution Methodology

In view of the following transformations

$$T = T_\infty \left(1 + (\Theta_w - 1)\Theta(\eta)\right), \ \ \eta = \sqrt{\frac{\alpha e^{\frac{s}{d}}}{2dv}} r, \quad \mathrm{v} = \frac{\mathrm{R}^\circ}{r + \mathrm{R}^\circ} \sqrt{\frac{\alpha e^{\frac{s}{d}}}{2dv}} \left(\mathrm{f}(\eta) + \eta \mathrm{f}'(\eta)\right),$$

$$\mathrm{N} = \alpha \sqrt{\frac{\alpha e^{\frac{s}{d}}}{2dv}} e^{\frac{s}{d}} \mathrm{g}(\eta), \ \ p = \rho \alpha^2 e^{\frac{s}{d}} \mathrm{P}(\eta), \ \ u = \alpha e^{\frac{s}{d}} \mathrm{f}'(\eta), \ \ \Theta_w = \frac{T_w}{T_\infty}. \tag{9}$$

Eqs. (2) to (8), become

$$\frac{dP}{d\eta} = \frac{1}{(\omega+\eta)} \left(\frac{df}{d\eta}\right)^2, \tag{10}$$

$$\frac{\omega\eta}{(\omega+\eta)} \frac{dP}{d\eta} + \frac{4\omega}{(\omega+\eta)} P = (1+\beta) \left(\frac{d^3 f}{d\eta^3} + \frac{1}{(\omega+\eta)} \frac{d^2 f}{d\eta^2} - \frac{1}{(\omega+\eta)^2} \frac{df}{d\eta}\right)$$

$$- \frac{2\omega}{(\omega+\eta)} \left(\frac{df}{d\eta}\right)^2 + \frac{\omega\eta}{(\omega+\eta)^2} \left(\frac{df}{d\eta}\right)^2 + \frac{\omega}{(\omega+\eta)} f \frac{d^2 f}{d\eta^2}$$

$$+ \frac{\omega}{(\omega+\eta)^2} f \frac{df}{d\eta} - \beta \frac{dg}{d\eta} - M \frac{df}{d\eta}, \tag{11}$$

$$\left(1 + \frac{\beta}{2}\right) \left[\frac{d^2 g}{d\eta^2} + \frac{1}{(\omega+\eta)} \frac{dg}{d\eta}\right] + \frac{\omega}{(\omega+\eta)} \left(f \frac{dg}{d\eta} - g \frac{df}{d\eta}\right) - \beta \left(2g + \frac{d^2 f}{d\eta^2} + \frac{1}{(\omega+\eta)} \frac{df}{d\eta}\right), \tag{12}$$

$$(1 + \varepsilon\Theta) \left[\frac{d^2\Theta}{d\eta^2} + \frac{1}{(\omega+\eta)} \frac{d\Theta}{d\eta} + \hat{A} \frac{df}{d\eta} + \hat{B}\Theta\right] + \varepsilon \left(\frac{d\Theta}{d\eta}\right)^2 + Pr \frac{\omega}{(\omega+\eta)} f \frac{d\Theta}{d\eta}$$

$$+\gamma\left(\frac{\omega}{\omega+\eta}\right)^2\left[\begin{matrix}f^2\frac{d^2\Theta}{d\eta^2}+\frac{1}{(\omega+\eta)}\frac{d\Theta}{d\eta}\frac{df}{d\eta}\left(f+\eta\frac{df}{d\eta}\right)\\+\frac{d\Theta}{d\eta}\left(f+\eta\frac{df}{d\eta}\right)\left(2\frac{df}{d\eta}-\eta\frac{df}{d\eta}\right)\end{matrix}\right], \tag{13}$$

where

$$Pr=\frac{\mu c_p}{k_\infty},\omega=\sqrt{\frac{\frac{s}{d}}{\alpha e 2dv}}R^*,\ M=\frac{\sigma\vec{B}2d}{\alpha\rho},\ \beta=\frac{\breve{k}}{\upsilon},\ \gamma=\lambda\alpha,\ \varepsilon=c(T_w-T_\infty), \tag{14}$$

In which M is the magnetic field, ε is the thermal conductivity parameter, Pr is the Prandtl number, ω is the curvature factor, β is the material parameter, and γ is the thermal relaxation time.

The boundary condition can be written as

$$f(0)=0,\Theta'(0)=-Bi\big(1-\Theta(0)\big),f'(0)=1,g(0)=-M_r f''(0),$$

$$f'(\infty)\to 0,\ \theta(\infty)\to 0,\ f''(\infty)\to 0,\ g(\infty)\to 0, \tag{15}$$

where

$$Bi=\frac{hd}{k_\infty}, \tag{16}$$

where h is heat transfer, Bi is Biot number.

After eliminating the pressure term from Eqs. (10) and (11), we get

$$\begin{aligned}(1+\beta)\left(\frac{d^4f}{d\eta^4}+\frac{2}{(\omega+\eta)}\frac{d^3f}{d\eta^3}-\frac{1}{(\omega+\eta)^2}\frac{d^2f}{d\eta^2}+\frac{1}{(\omega+\eta)^3}\frac{df}{d\eta}\right)-\omega\left(\frac{d^2g}{d\eta^2}+\frac{dg}{d\eta}\right)\\+\frac{\omega}{(\omega+\eta)}\left(f\frac{d^3f}{d\eta^3}+\frac{df}{d\eta}+f\frac{df}{d\eta}+f\frac{d^2f}{d\eta^2}\right)-M\left(\frac{df}{d\eta}+\frac{f}{(\omega+\eta)}\right)\\+\frac{1}{(\omega+\eta)}\left(\frac{df}{d\eta}\right)^2\left[\frac{-4}{(\omega+\eta)}-\frac{\omega}{(\omega+\eta)^2}+\frac{\omega}{(\omega+\eta)}-\omega\right]\end{aligned}$$

$$+\frac{2}{(\omega+\eta)}\frac{d^2f}{d\eta^2}\left(\frac{\omega}{(\omega+\eta)}-\eta\omega-2\right)=0\,. \tag{17}$$

The skin friction, couple stress, and Nusselt number are given as:

$$C_f=\frac{\tau_w}{\frac{1}{2}\rho(u_w)^2},\ \ C_s=\frac{M_w}{\mu j u_w},\ Nu=\frac{s j_w}{k_\infty(T_w-T_\infty)}. \tag{18}$$

Eq. (18) in non-dimensional form can be written as:

$$Re^{\frac{1}{2}}C_f = 2\left((1+\beta)\left(\frac{d^2f}{d\eta^2} - \frac{1}{\beta}\frac{df}{d\eta}\right)_{\eta=0} - \beta M_r\left(\frac{d^2f}{d\eta^2}\right)_{\eta=0}\right),$$

$$C_s = \left(1+\frac{\beta}{2}\right)\left(\frac{dg}{d\eta}\right)_{\eta=0}, Re^{-\frac{1}{2}}Nu = -(1+N_r\Theta_w^3)\left(\frac{d\Theta}{d\eta}\right)_{\eta=0}, \quad (19)$$

where $Re = \frac{u_w(s)}{v}$ is Reynolds number.

4. Result and Discussion

This research investigates the impact of various parameters on a magnetohydrodynamic (MHD) micropolar fluid flow, specifically focusing on the role of variable thermal conductivity and the Cattaneo-Christov heat flux model over an exponentially extended curved stretching surface. The study uses graphical illustrations to analyze the effects of key parameters on velocity, temperature, and other relevant flow characteristics. These graphical representations help visualize the influence of parameters like the magnetic field, thermal relaxation time, and the nature of the stretching surface on the fluid's behaviour. The effect of magnetic field M on velocity distribution $f'(\eta)$ is shown in Fig. 2. It is observed that when value of the M rises, the velocity is reduced. It is because of magnetic force which produces the resistance in the direction of flow. Fig. 3 describes the influence of microrotation parameter M_r on the velocity distribution $f'(\eta)$. It is noted that the velocity decreases by increasing values of M_r . Fig. 4 describes the influence of material parameter β on the velocity distribution $f'(\eta)$, which shows that by increasing β, the velocity also increases. It is in accordance with the physical expectation because β is inversely proportional to viscosity, as viscosity decreases, the thickness of the boundary layer also decreases. Fig. 5 portrays the influence of curvature ω on velocity $f'(\eta)$. It is noted that by raising the curvature values, the velocity also grows because the radius of the exponential surface expands, which causes an increase in velocity. To show the influence of magnetic force on microrotation Fig. 6 is generated, which shows that when the values of M is enhanced then the microrotation distribution g(η) decreases. It is due to the Lorentz force caused by magnetic field, which produces disturbance in the flow. Fig. 7 depicts the effects of microrotation parameter M_r on g(η). It is perceived that when values of M_r increases, the microrotation distribution also rises. In Fig. 8, the effects of material parameter β on microrotation has been displayed. It is seen that as β increases, g(η) also increases. The reason for this is that boundary layer thickness declines as viscosity decreases because β and viscosity are inversely proportional. Fig. 9 describes the effects of magnetic parameter M on θ(η). It is observed that the temperature rises for increasing values of magnetic parameter M. Fig. 10 describes how the Prandtl number affects the temperature distribution. The temperature decreases for rising values of Pr. Basically, Pr is the ratio between thermal diffusivity and momentum diffusivity, consequently the temperature and the boundary layer thickness both reduce when Pr increases. Fig. 11 shows how an increase in B values affects temperature θ(η). It is perceived that the temperature rises due to the presence of irregular heat component. Fig. 12 is plotted to show the impact of curvature ω on the temperature θ(η). The temperature decreases when curvature values rises because the radius of the exponential surface increases, as a matter of facts, the temperature distribution reduces. The impact of thermal conductivity ε on the temperature is shown Fig. 13. It is noticed that when thermal conductivity increases, temperature also rises.

Tables 1 and 2 analyze the numerical results of skin friction and couple stress for various values of M, ω, and β. From Table 1, it is clear that skin friction reduces by increasing the value of curvature, whereas as reverse impact is observed for rising values of M and β, that is skin friction increases. In Table 2, it is found that the couple stress coefficient increases when values of M and β rise, ω is fixed. Table 3 illustrates the rate at which heat transfer increases with rising values of Pr and γ. Table 4 shows the comparison of skin friction of the existing work with Alqahtani et al. [35] and found in good agreement.

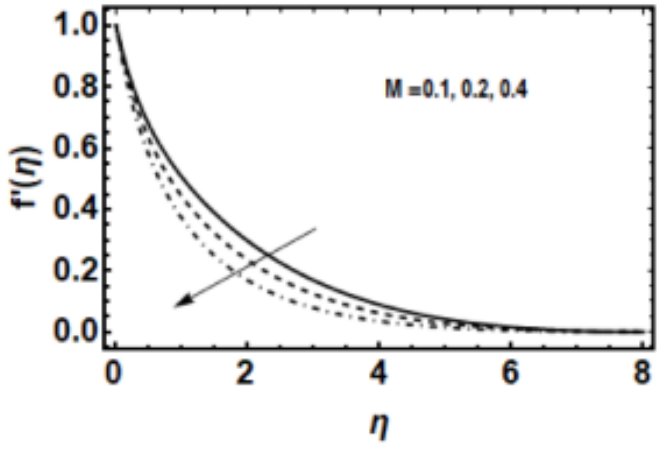

Fig 2: Velocity for several values of M.

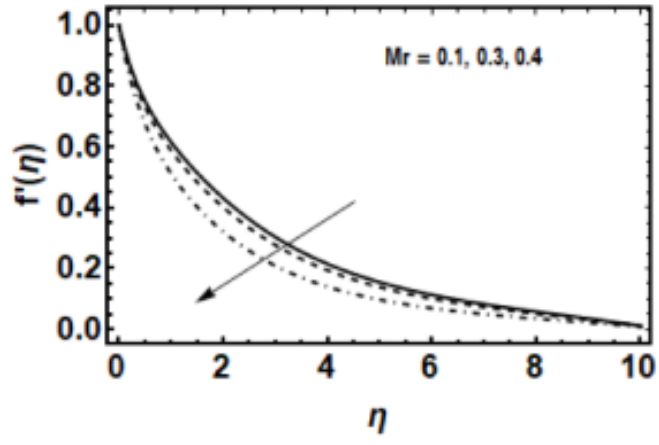

Fig 3: Velocity for several values of M_r.

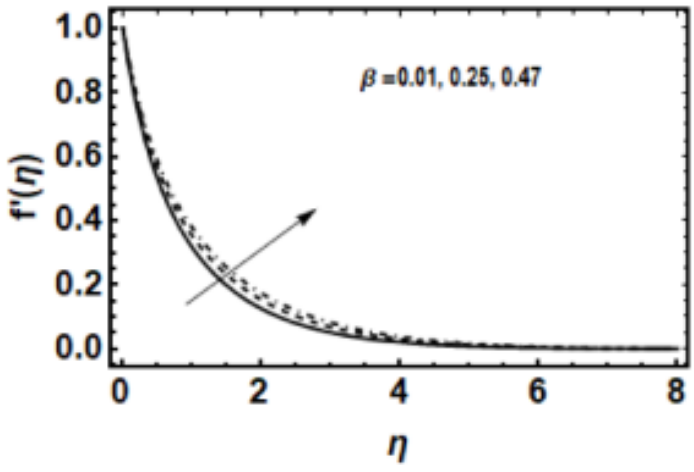

Fig 4: Velocity for several values of β.

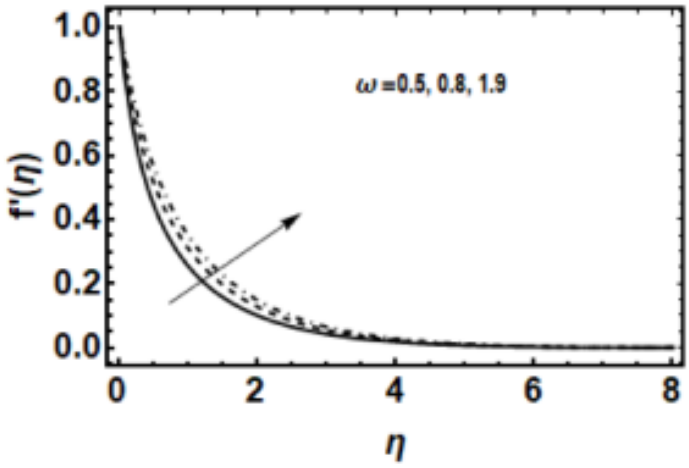

Fig 5: Velocity for several values of curvature.

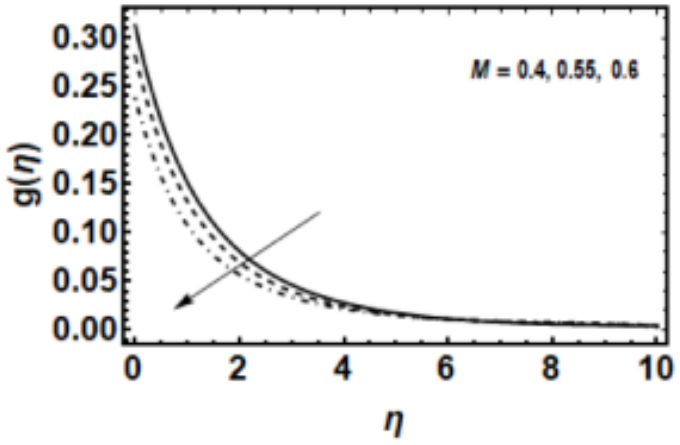

Fig 6: Effect of M on microrotation.

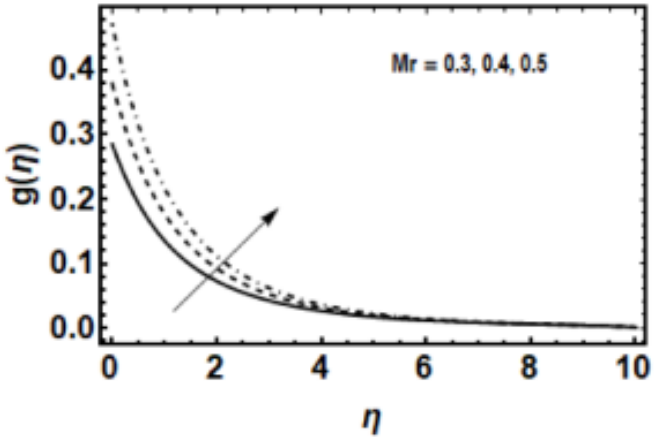

Fig 7: Effect of M_r on microrotation.

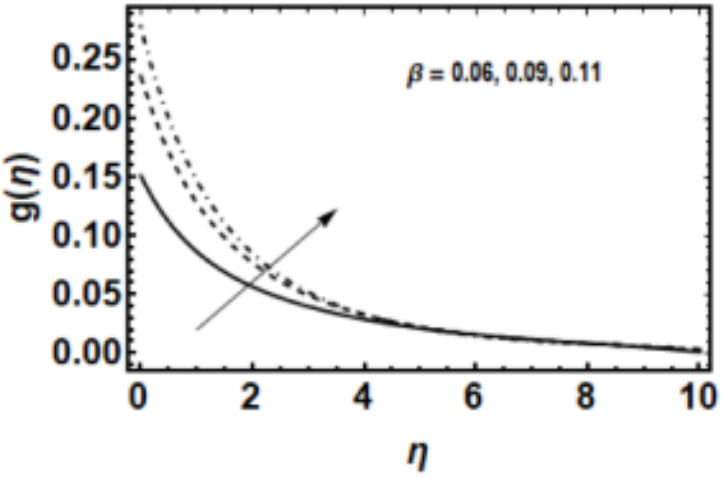

Fig 8: Effect of β on micro rotation.

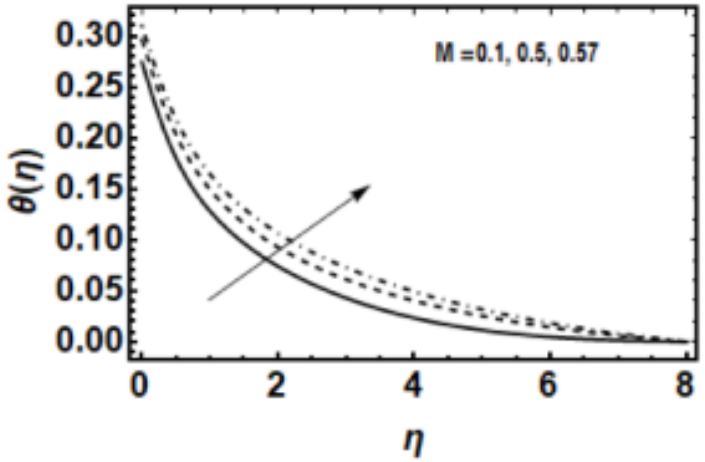

Fig 9: Temperature for several values of M.

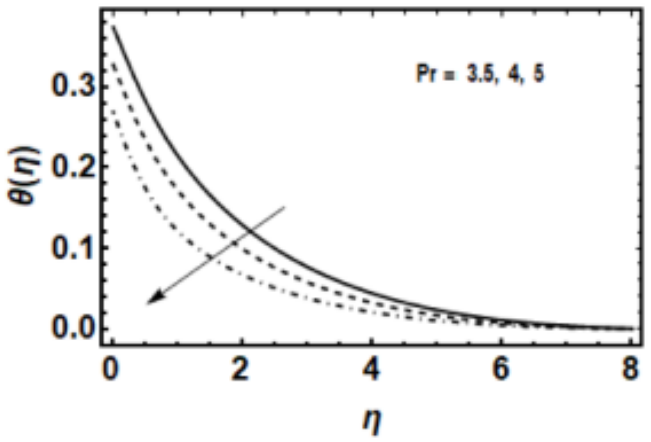

Fig 10: Temperature for several values of Pr.

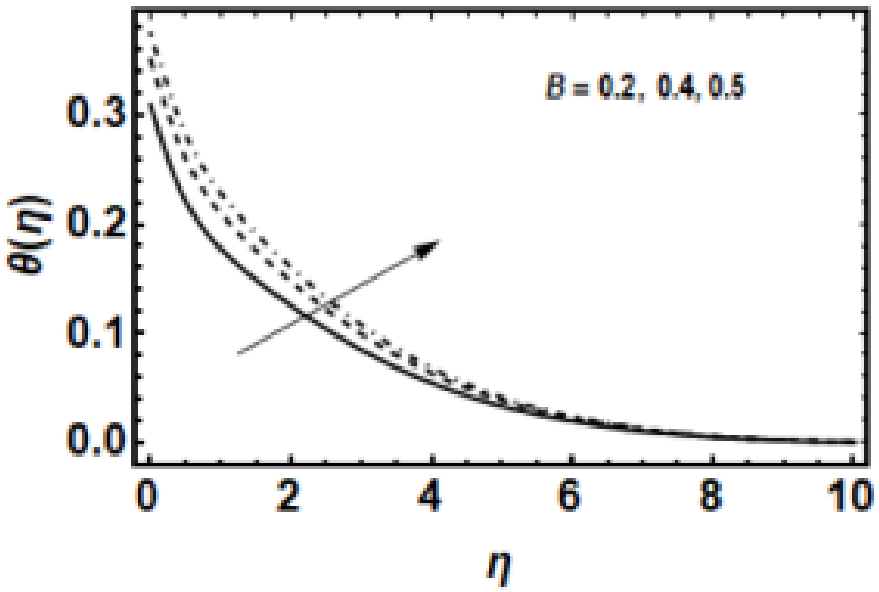

Fig 11: Temperature for several values of $\hat{B}$.

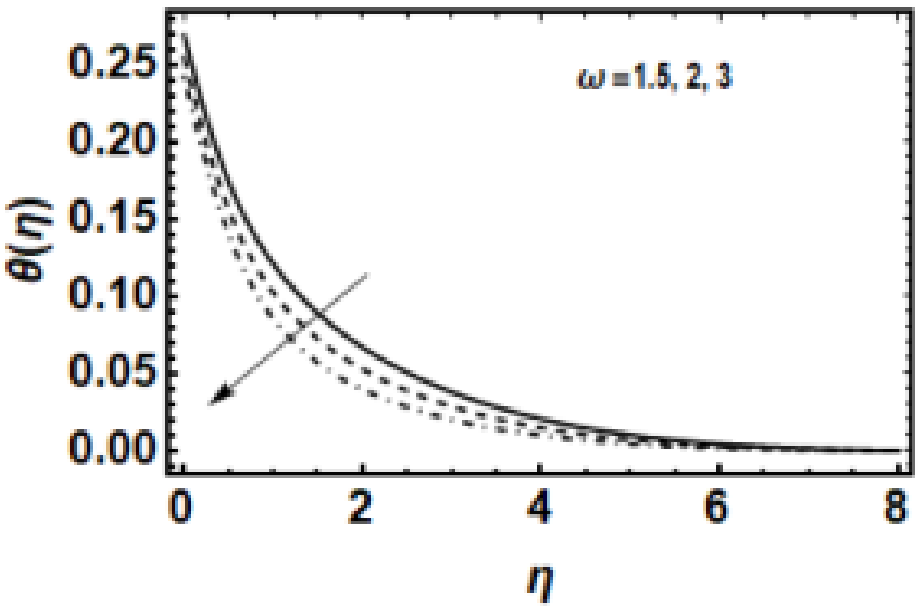

Fig 12: Temperature for several values of curvature ω.

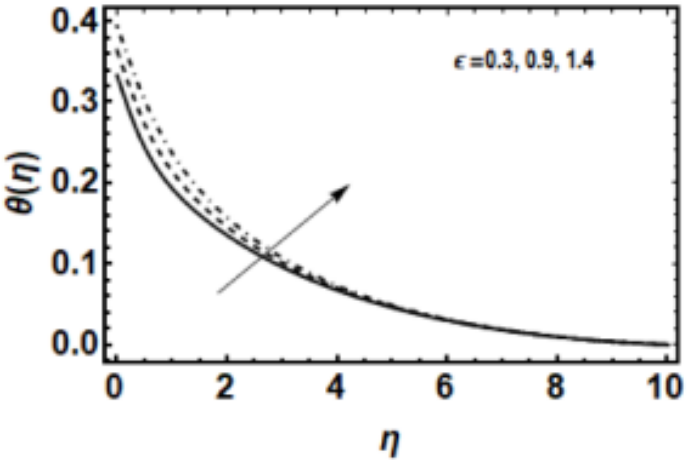

Fig 13: Temperature for several values of thermal conductivity parameter.

Table 1: Value of $-Re^{\frac{1}{2}}C_f$ when Pr =3 and γ =0.7

Ω	B	M	$-Re^{\frac{1}{2}}C_f$
1.5	0.6	0.9	0.74651
1.8			O.65943
0.5			0.58972
1.8	0.5	0.5	0.45853
	0.6		0.63018
	0.9		0.78699
1.8	0.6	0.9	0.65943
		1.1	0.70581
		1.6	0.73219

5. Conclusions

Key points of this investigation include:

➢ Increasing the magnetohydrodynamic (MHD) leads to a decrease in fluid velocity and microrotation distribution, while the temperature profile increases. This is because the Lorentz force, generated by the magnetic field, opposes the

fluid motion, thus reducing velocity. The increased temperature is a result of the energy dissipation caused by the Lorentz force and the magnetic field.

- Increasing the Prandtl number in a fluid flow leads to a reduction in the temperature profile. This is because a higher Prandtl number indicates a fluid with a lower thermal diffusivity, meaning heat diffuses more slowly compared to momentum. Consequently, the thermal boundary layer, which is the region where temperature changes significantly, becomes thinner, resulting in a lower overall temperature distribution.
- Increasing the material parameter leads to a decrease in fluid velocity while causing an increase in microrotation. This behavior is attributed to the relationship between the material parameter and the fluid's microstructure, where a higher material parameter implies a greater resistance to deformation and thus a reduction in overall flow speed. Conversely, the increased resistance is due to the material parameter also enhances the microrotation, which represents the local angular momentum of the fluid particles.
- It is observed that as the curvature parameter increases, the velocity profile tends to increase, while the temperature decreases. This is because a higher curvature parameter reduces the contact surface area, leading to less resistance to fluid flow and thus increasing velocity. Simultaneously, the increased flow velocity leads to a decrease in temperature due to the reduced viscous dissipation.

Table 2: Value of couple stress when ω=1.

B	**M**	**Re_sC_m**
0.4	0.5	0.01343
0.6		0.01368
1.2		0.01881
0.9	0.7	0.01767
	0.8	0.01838
	0.9	0.01904

Table 3: Value of heat Transfer rate when ω=1 and β=0.

γ	**Pr**	**- $\theta'(0)$**
0.1	3	0.134224
0.15		0.14618
0.2		0.15352
0.1	1	0.31660
	1.5	0.48672
	2	0.57226

Table 4: Comparison of skin friction of the present work with published work.

β	Alqahtani et al. [34]	Present Study
0.5	1.52075	1.52054
1	1.45782	1.45745
1.5	1.42466	1.42479
2	1.41392	1.41368
2.5	1.30860	1.30852
3	1.30558	1.30565

Acknowledgment. Dr Sultan Z Alamri express gratitude to Taibah University Madinah for support.

References

[1] M. M. Bhatti, A. Zeeshan, F. Bashir, S. M. Sait, R. Ellahi, Sinusoidal motion of small particles through a Darcy-Brinkman-Forchheimer microchannel filled with non-Newtonian fluid under electro-osmotic forces, *Journal of Taibah University for Science,* Vol. 15, No. 1, pp. 514-529, 2021/01/01, 2021.
[2] F. Ishtiaq, R. Ellahi, M. M. Bhatti, S. Z. Alamri, Insight in Thermally Radiative Cilia-Driven Flow of Electrically Conducting Non-Newtonian Jeffrey Fluid under the Influence of Induced Magnetic Field, *Mathematics,* Vol. 10, No. 12, pp. 2007, 2022.
[3] A. A. Khan, B. Zahra, R. Ellahi, S. M. Sait, Analytical Solutions of Peristalsis Flow of Non-Newtonian Williamson Fluid in a Curved Micro-Channel under the Effects of Electro-Osmotic and Entropy Generation, *Symmetry,* Vol. 15, No. 4, pp. 889, 2023.
[4] R. Ellahi, The effects of MHD and temperature dependent viscosity on the flow of non-Newtonian nanofluid in a pipe: Analytical solutions, *Applied Mathematical Modelling,* Vol. 37, No. 3, pp. 1451-1467, 2013/02/01/, 2013.
[5] F. Ishtiaq, R. Ellahi, M. M. Bhatti, S. Sait, Convective heat transfer with Hall current using magnetized non-Newtonian Carreau fluid model on the cilia-attenuated flow, *International Journal of Numerical Methods for Heat & Fluid Flow,* Vol. 34, 07/16, 2024.
[6] S. M. Sait, R. Ellahi, N. Khalid, T. Taha, A. Zeeshan, Effects of thermal radiation on MHD bioconvection flow of non-Newtonian fluids using linear regression based machine learning and artificial neural networks, *International Journal of Numerical Methods for Heat & Fluid Flow,* Vol. 35, No. 5, pp. 1587-1609, 2025.
[7] M. S. Nadeem, A. Zeeshan, A. Majeed, S. M. Sait, R. Ellahi, Cavitating bubbly flow of non-Newtonian second grade fluid through nozzles: Application of reduction of cavitation damage and noise, *International Journal of Modern Physics B,* Vol. 39, No. 11, pp. 2550085, 2025.
[8] R. Ellahi, A. Zeeshan, S. Shafique, S. M. Sait, A. u. Rehman, Electroosmotic slip flow in peristaltic transport of non-Newtonian third-grade MHD fluid: RSM-based sensitivity analysis, *International Journal of Heat and Mass Transfer,* Vol. 247, pp. 127121, 2025/09/01/, 2025.
[9] A. C. Eringen, Simple microfluids, *International Journal of Engineering Science,* Vol. 2, No. 2, pp. 205-217, 1964/05/01/, 1964.
[10] A. C. Eringen, Theory of Micropolar Fluids, *Journal of Mathematics and Mechanics,* Vol. 16, No. 1, pp. 1-18, 1966.
[11] C. Eringen, 1970, *Foundations of Micropolar Thermoelasticity*, Springer Vienna,
[12] A. A. Khan, S. M. Sait, R. Ellahi, Reflection of Harmonic Waves in a Nonlocal Rotating Micropolar Medium with Constant Magnetic Field under Three-phase-lag Theory with Temperature Dependent Elastic Model, *Journal of Computational Applied Mechanics,* Vol. 56, No. 2, pp. 331-344, 2025.

[13] M. Turkyilmazoglu, Flow of a micropolar fluid due to a porous stretching sheet and heat transfer, *International Journal of Non-Linear Mechanics,* Vol. 83, pp. 59-64, 2016/07/01/, 2016.
[14] Seyed M. Hashem Zadeh, S. A. M. Mehryan, M. A. Sheremet, M. Izadi, M. Ghodrat, Numerical study of mixed bio-convection associated with a micropolar fluid, *Thermal Science and Engineering Progress,* Vol. 18, pp. 100539, 2020/08/01/, 2020.
[15] A. Sid Ahmed, B. Ayoub, B. M. Najib, B. A. Manal, Conjugate Mixed Convection of a Micropolar Fluid Over a Vertical Hollow Circular Cylinder, *International Journal of Applied Mechanics and Engineering,* Vol. 29, No. 1, pp. 1-18, 2024.
[16] N. S. Elgazery, N. Y. Abd Elazem, Insights into viscosity/thermal conductivity of a micropolar nanofluid flow near a horizontal cylinder, *Journal of Nanofluids,* Vol. 13, No. 2, pp. 614-624, 2024.
[17] M. Ghobadi, Y. S. Muzychka, A Review of Heat Transfer and Pressure Drop Correlations for Laminar Flow in Curved Circular Ducts, *Heat Transfer Engineering,* Vol. 37, No. 10, pp. 815-839, 2016/07/02, 2016.
[18] A. Afsar Khan, R. Batool, N. Kousar, Examining the behavior of MHD micropolar fluid over curved stretching surface based on the modified Fourier law, *Scientia Iranica,* Vol. 28, No. 1, pp. 223-230, 2021.
[19] T. Muhammad, K. Rafique, M. Asma, M. Alghamdi, Darcy–Forchheimer flow over an exponentially stretching curved surface with Cattaneo–Christov double diffusion, *Physica A: Statistical Mechanics and its Applications,* Vol. 556, pp. 123968, 2020/10/15/, 2020.
[20] A. K. Kempannagari, R. R. Buruju, S. Naramgari, S. Vangala, Effect of Joule heating on MHD non-Newtonian fluid flow past an exponentially stretching curved surface, *Heat Transfer,* Vol. 49, No. 6, pp. 3575-3592, 2020.
[21] Q.-H. Shi, T. Shabbir, M. Mushtaq, M. I. Khan, Z. Shah, P. Kumam, Modelling and numerical computation for flow of micropolar fluid towards an exponential curved surface: a Keller box method, *Scientific Reports,* Vol. 11, No. 1, pp. 16351, 2021/08/11, 2021.
[22] K. A. Kumar, V. Sugunamma, N. Sandeep, S. Sivaiah, Physical Aspects on MHD Micropolar Fluid Flow Past an Exponentially Stretching Curved Surface, *Defect and Diffusion Forum,* Vol. 401, pp. 79-91, 2020.
[23] R. Ellahi, A. Zeeshan, N. Shehzad, S. Z. Alamri, Structural impact of kerosene-Al2O3 nanoliquid on MHD Poiseuille flow with variable thermal conductivity: Application of cooling process, *Journal of Molecular Liquids,* Vol. 264, pp. 607-615, 2018/08/15/, 2018.
[24] A. A. Khan, S. Naeem, R. Ellahi, S. M. Sait, K. Vafai, Dufour and Soret effects on Darcy-Forchheimer flow of second-grade fluid with the variable magnetic field and thermal conductivity, *International Journal of Numerical Methods for Heat & Fluid Flow,* Vol. 30, No. 9, pp. 4331-4347, 2020.
[25] A. Kanwal, A. A. Khan, S. M. Sait, R. Ellahi, Heat transfer analysis of magnetohydrodynamics peristaltic fluid with inhomogeneous solid particles and variable thermal conductivity through curved passageway, *International Journal of Numerical Methods for Heat & Fluid Flow,* Vol. 34, No. 4, pp. 1884-1902, 2024.
[26] A. Khan, S. Noor, R. Ellahi, S. Sait, THERMAL ANALYSIS OF TWO-PHASE MHD FLOW DUE TO CILIARY MOVEMENT WITH VISCOUS DISSIPATION IN THE PRESENCE OF HEAT SOURCE/SINK, *Journal of Enhanced Heat Transfer*, 01/01, 2025.
[27] A. M. Megahed, M. G. Reddy, W. Abbas, Modeling of MHD fluid flow over an unsteady stretching sheet with thermal radiation, variable fluid properties and heat flux, *Mathematics and Computers in Simulation,* Vol. 185, pp. 583-593, 2021/07/01/, 2021.
[28] A. A. Khan, S. Ilyas, T. Abbas, R. Ellahi, Significance of induced magnetic field and variable thermal conductivity on stagnation point flow of second grade fluid, *Journal of Central South University,* Vol. 28, No. 11, pp. 3381-3390, 2021/11/01, 2021.
[29] S. Z. Alamri, A. A. Khan, M. Azeez, R. Ellahi, Effects of mass transfer on MHD second grade fluid towards stretching cylinder: A novel perspective of Cattaneo–Christov heat flux model, *Physics Letters A,* Vol. 383, No. 2, pp. 276-281, 2019/01/12/, 2019.
[30] A. A. Khan, I. Saleem, R. Ellahi, S. M. Sait, K. Vafai, On magnetohydrodynamics Powell–Eyring fluid with Cattaneo–Christov heat flux over a curved surface, *International Journal of Modern Physics B,* Vol. 37, No. 19, pp. 2350190, 2023.
[31] J. Mehboob, R. Ellahi, S. M. Sait, N. S. Akbar, Optimizing bioconvective heat transfer with MHD Eyring–Powell nanofluids containing motile microorganisms with viscosity variability and porous media in ciliated microchannels, *International Journal of Numerical Methods for Heat & Fluid Flow,* Vol. 35, No. 2, pp. 825-846, 2025.
[32] A. Zeeshan, N. Khalid, R. Ellahi, M. Khan, S. Z. Alamri, Analysis of nonlinear complex heat transfer MHD flow of Jeffrey nanofluid over an exponentially stretching sheet via three phase artificial intelligence and Machine Learning techniques, *Chaos, Solitons & Fractals,* Vol. 189, pp. 115600, 2024.

[33] R. Ellahi, S. Alamri, A. Majeed, Effects of MHD and slip on heat transfer boundary layer flow over a moving plate based on specific entropy generation, *Journal of Taibah University for Science,* Vol. 12, pp. 1-7, 06/14, 2018.

[34] A. M. Alqahtani, Zeeshan, W. Khan, Amina, S. A. Alhabeeb, H. A. El-Wahed Khalifa, Stability of magnetohydrodynamics free convective micropolar thermal liquid movement over an exponentially extended curved surface, *Heliyon,* Vol. 9, No. 11, 2023.